PAIRWISE ADVERSARIAL TRAINING FOR UNSUPERVISED CLASS-IMBALANCED DOMAIN ADAPTATION

Anonymous authors
Paper under double-blind review

ABSTRACT

Unsupervised domain adaptation (UDA) has become an appealing approach for knowledge transfer from a labeled source domain to an unlabeled target domain. However, when the classes in source and target domains are imbalanced, most existing UDA methods experience significant performance drop, as the decision boundary usually favors the majority classes. Some recent class-imbalanced domain adaptation (CDA) methods aim to tackle the challenge of biased label distribution by exploiting pseudo-labeled target data during training process. However, these methods still suffer from the issues with unreliable pseudo labels and error accumulation during training. In this paper, we propose a pairwise adversarial training approach for class-imbalanced domain adaptation. Unlike conventional adversarial training in which the adversarial samples are obtained from the ℓ_p ball of the original data, we generate adversarial samples from the interpolated line of the aligned pairwise samples from source domain and target domain. Experimental results and ablation studies show that our method achieves considerable improvements on benchmarks compared with the state-of-art CDA methods.

‘

1 INTRODUCTION

Unsupervised domain adaptation (UDA) aims to achieve knowledge transfer from a labeled source domain to an unlabelled target domain. Recent years have witnessed the significant progress of UDA based on deep neural networks. Most of existing UDA methods assume that only covariate shift occurs in the source domain and target domain, while the label distributions in two domains are identical. However, this assumption may not hold in real-world applications. For instance, in wild-life pictures, the commonly seen animals such as rabbit and deer appear more frequently than the rare animal such as panda and crocodile. Public datasets such as DomainNet (Peng et al., 2019), LVIS (Gupta et al., 2019) and MSCOCO (Lin et al., 2014) also exhibit imbalanced class distribution. Figure 1 illustrates the imbalanced label distributions in the *Real* domain and *Sketch* domain from the DomainNet dataset.

To address the issue of imbalanced label distributions in domain adaptation, some recent studies try to jointly model the conditional feature distribution shift and label distribution shift (LDS). This problem is referred to as Class-imbalanced Domain Adaptation (CDA). Let x and y denote the samples and labels, respectively. p and q separately represent the probability distribution of source domain and target domain. The common assumptions in UDA involve the covariate shift (i.e., $p(x) \neq q(x)$) and identical label distribution (i.e., $p(y) = q(y)$). In CDA, however, apart from the covariate shift, both the conditional feature shift and label shift exist, i.e., $p(x|y) \neq q(x|y), p(y) \neq q(y)$.

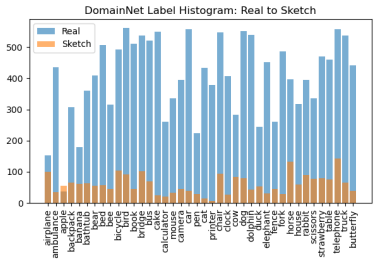

Figure 1: Illustration of label distribution shift in DomainNet dataset.

CDA is a more challenging task than UDA. Recent studies have demonstrated that the mainstream UDA methods will suffer significant performance drop, as the classifier will favor the majority

classes (Tan et al., 2020). Only a few CDA approaches have been proposed by far. In (Tan et al., 2020), the negative effect of label shift is reduced by exploiting the pseudo labelled target samples via self-training. Jiang et al. (2020) use an implicit sampling method based on pseudo labels to align the joint distribution between features and labels. However, one critical problem of these methods is that the pseudo labels are likely to suffer from ill-calibrated probabilities (Guo et al., 2017), and thus the unreliable pseudo labels will cause error accumulation during the training process, which will largely degrade the model performance.

Augmenting training data has been proven as an effective strategy to tackle the issue of biased label distributions in class-imbalance learning (Chawla et al., 2002; Chou et al., 2020). In addition to the traditional data augmentation techniques, adversarial training is also capable of generating semantically meaningful synthetic samples that help enhance the robustness of models. However, these approaches only consider a single domain, and they cannot be directly applied to solve the CDA problem. In this paper, we propose a pairwise adversarial training (PAT) approach that augments training data for class-imbalanced domain adaptation. Unlike conventional adversarial training in which the adversarial samples are obtained from the ℓ_p ball of the original data, we obtain the semantic adversarial samples from the interpolated line of the aligned pair-wise samples from source domain and target domain. Moreover, a class-imbalanced semantic centroid alignment strategy is designed to explicitly align the source and target domains in the feature space.

The main contributions of this paper are three-fold. (1) We propose a novel pairwise adversarial training approach that generates adversarial samples from pairs of samples across the source and target domains, and further exploits these samples to augment training data. (2) We propose a new optimization algorithm to solve pairwise adversarial training problem. (3) We conduct extensive evaluations on benchmark datasets, and results show that our approach obtains competing performance compared with state-of-art CDA methods.

2 Related Work

In this section, we briefly introduce three relevant research topics, including unsupervised domain adaptation, class-imbalanced domain adaptation and adversarial training.

Unsupervised Domain Adaptation. In recent years, unsupervised domain adaption (UDA) has attracted increasing attention. Existing UDA methods could be roughly categorized into two groups, including the discrepancy-based methods and adversarial-based methods. The discrepancy-based methods usually align source and target feature distributions in the embedding space using various statistical distance metrics, such as Maximum Mean Discrepancy (MMD) (Long et al., 2016; 2017; Kang et al., 2019), Correlation Alignment (CORAL) (Sun & Saenko, 2016), and Wasserstein distance (Lee & Raginsky, 2018; Shen et al., 2018; Balaji et al., 2019). On the other hand, the adversarial-based methods focus on learning domain invariant features via domain adversarial training (Ganin et al., 2016; Shu et al., 2018; Pei et al., 2018; Saito et al., 2018; Deng et al., 2019; Yu et al., 2019). Recently, Zhang et al. (2019) proposed the margin disparity discrepancy (MDD) to measure the discrepancy of two domains with generalization bounds. This theory is tailored into an adversarial learning algorithm for domain adaptation. Unlike other adversarial learning based UDA methods that align two domains by confusing a domain discriminator, MDD aligns two domains by minimizing the maximum margin disparity discrepancy of an optimal classifier f and an auxiliary classifier f'. The optimization problem of MDD is formulated as:

$$\min_{f,\psi} \varepsilon(\mathcal{D}_s) + \eta \mathcal{D}_\gamma(\mathcal{D}_s, \mathcal{D}_t), \tag{1}$$

$$\max_{f'} \mathcal{D}_\gamma(\mathcal{D}_s, \mathcal{D}_t), \tag{2}$$

where ε is the classification loss on the source domain and $\mathcal{D}_\gamma$ measures the discrepancy of source domain and target domain. Specifically,

$$\varepsilon(\mathcal{D}_s) = \mathbb{E}_{(x^s,y^s)\sim\mathcal{D}_s} \mathcal{L}(f(\psi(x^s)), y^s), \tag{3}$$

$$\mathcal{L}_{adv} = \mathcal{D}_\gamma(\mathcal{D}_s, \mathcal{D}_t) = \mathbb{E}_{x^t\sim\mathcal{D}_t} \mathcal{L}'(f'(\psi(x^t)), f(\psi(x^t))) - \gamma \mathbb{E}_{x^s\sim\mathcal{D}_s} \mathcal{L}(f'(\psi(x^s))), f(\psi(x^s)), \tag{4}$$

$\mathcal{L}$ is cross-entropy function, and $\mathcal{L}'(f'(\psi(x^t)), f(\psi(x^t))) = \log(1 - \sigma_{y'}(f'(\psi(x^t)))$. y' is the pseudo label generated from an optimal classifier. MDD is the backbone of our method.

Class-imbalanced Domain Adaptation. As a branch of domain adaptation, the class-imbalanced domain adaptation (CDA) aims to deal with data with biased class distribution. Tan et al. (2020) might be the first one to investigate the CDA problem, and they exploited the pseudo labelled target data to reduce the negative effect of label shift. Wu et al. (2019) proposed the asymmetrically-relaxed distances as replacement of the standard ones under the biased label distribution. Jiang et al. (2020) adopted the implicit sampling strategy to ensure class alignment at the minibatch level. Prabhu et al. (2021) avoided the use of highly unreliable pseudo labels by assessing the reliability of target data based on the predictive consistency under a series of random image transformations. In our method, we refrain from the exploitation of pseudo labelled target data directly in the training process, while reducing the effect of biased label shift by incorporating the semantic adversarial samples into the training process.

Adversarial Training. Adversarial training (AT) (Szegedy et al., 2014; Goodfellow et al., 2015) is an effective regularization method for enhancing the robustness and generalization ability of deep learning models. In particular, adversarial samples are incorporated in the model training process, which are intentionally designed to deceive the deep learning model by adding small perturbation on the original data. Furthermore, virtual adversarial training (VAT) has been proposed (Miyato et al., 2018), which seeks the adversarial direction for regularization without using label information. Both AT and VAT have been employed to tackle the standard UDA problems Shu et al. (2018). However, to the best of our knowledge, our work is the first attempt to address the class-imbalanced domain adaptation problem using adversarial training.

3 Proposed Approach

In this section, we first give the problem definition of CDA and define mathematical notations used throughout this paper. We then present the details of the proposed pairwise adversarial training approach, and finally introduce how to integrate the pairwise adversarial training with MDD to address the CDA problem.

3.1 Problem Definition

In class-imbalanced domain adaptation, both the source domain and target domain suffer from label distribution shift. We are given a source domain $\mathcal{D}_s = \{(x_i^s, y_i^s)\}_{i=1}^{N_s}$ with N^s labelled samples and a target domain $\mathcal{D}_t = \{x_i^t\}_{i=1}^{N_t}$ with N^t unlabelled samples. Each domain contains K classes, and the class label is denoted as $y^s \in \{0, 1, 2, ..., K-1\}$. Let p and q denote the probability distributions of the source domain and target domain, respectively. We assume that both the covariate shift (i.e., $p(x) \neq q(x)$) and label distribution shift (i.e., $p(y) \neq q(y)$ and $p(x|y) \neq q(x|y)$) exist in two domains. Our goal is to train a model that can learn domain invariant features, reduce the gap between source and target domains, and meanwhile mitigate the label distribution shift. The model typically consists of a feature extractor $\psi : \mathcal{X} \to \mathcal{Z}$ and a classifier $f : \mathcal{Z} \to \mathcal{Y}$ that aims to minimize the target risk.

3.2 Pairwise Adversarial Training (PAT)

We investigate how to mitigate the challenging issue of label distribution shift in CDA, as illustrated in Figure 1. An intuitive solution is to augment the training data in two domains, such that the model training would not be dominated by the majority classes in either domain. However, this task is not trivial, considering the mixed effects of domain gap and imbalanced class distributions. Inspired by adversarial training, we aim to create adversarial samples to augment training data. In adversarial training, the adversarial samples that maximize the loss function will be exploited to enhance the robustness and generalization ability of model. The loss function of adversarial training is:

$$\begin{aligned} &\mathcal{L}_{ce}(x + \delta^*, y; \theta) \\ \text{where} \quad &\delta^* := \underset{||\delta||_p \leq \epsilon}{\arg\max}\, \mathcal{L}_{ce}(x + \delta, y; \theta), \end{aligned} \tag{5}$$

where x is the original sample, y is the ground-truth label of x, θ refers to model parameters, and δ is the perturbation added to x.

The existing adversarial training methods could not be directly used to tackle the CDA problem for two reasons. First, existing methods simply generate adversarial samples within the neighborhood of the original samples, but they could not mitigate the gap between source and target domains. Second, existing methods treat majority classes and minority classes equally, so they are unable to address the class imbalance issue. In this paper, we propose pairwise adversarial training that generates adversarial samples from the linear interpolation of source and target samples and meanwhile reduces the domain discrepancy. In the following, we will introduce two key components of PAT, including the generation of interpolated adversarial samples and semantic centroid alignment.

3.2.1 INTERPOLATED ADVERSARIAL SAMPLE GENERATION

As shown in Figure 2, we will generate adversarial samples on the interpolated line from a source sample to a target sample of the same class. The interpolated adversarial samples should have the same semantic meaning as their corresponding source/target sample pair, although they are not perfectly aligned with the original samples. By augmenting the original data with interpolated adversarial samples, the model will generalize well on the imbalanced target domain. For the kth class, the interpolated adversarial samples can be defined as:

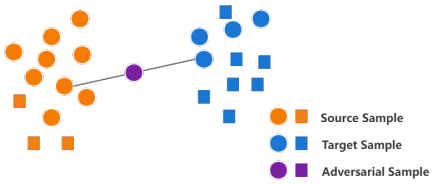

Figure 2: Illustration of an interpolated adversarial sample, which lies on the interpolated line of the source and target samples.

$$\mathcal{X}_k^{adv} = \{x_k^{adv} | x_i^{adv} = x_i^s + \lambda(x_i^t - x_i^s), \lambda \in [0,1)^C, y_i^s = \hat{y}_i^t = k\}, \tag{6}$$

where $x_i \in \mathbb{R}^{C\times H\times W}$, λ is the coefficient measuring the contributing weights of the source sample and target sample. $\hat{y}_i^t$ is the pseudo label of the target sample which is generated from the backbone domain adaptation model (e.g., the optimal classifier f in MDD). It is used for match of the corresponding source sample. In our work, we choose the target samples with high confidence.

Then, the generation of interpolated adversarial samples could be achieved by solving the following optimization problem:

$$\begin{aligned} &\mathcal{L}_{IAS} := D(\hat{x}^{adv}, y; \theta) \\ \text{where} \quad &\hat{x}^{adv} = \underset{x^{adv}\in\mathcal{X}^{adv}}{\arg\max}\ D'(x^{adv}, y; \theta). \end{aligned} \tag{7}$$

In Eq. (7), the outer minimization problem involves a standard cross-entropy loss function, i.e.,

$$D(\hat{x}^{adv}, y; \theta) = \mathcal{L}_{CE}(\hat{x}^{adv}, y; \theta) = -\log(\sigma_y(f(\psi(\hat{x}^{adv})))), \tag{8}$$

where $\psi : \mathcal{X} \to \mathcal{Z}$ denotes a feature extractor, $f : \mathcal{Z} \to \mathcal{Y}$ denotes a classifier, and σ is the softmax function. For the inner maximization problem, we use a modified cross-entropy function proposed by Goodfellow et al. (2014). The modified loss function can alleviate the problem of gradient exploding or vanishing when the entropy loss is maximized. The loss function of the inner maximization problem is written as:

$$D'(x^{adv}, y; \theta) = \mathcal{L}'_{CE}(x^{adv}, y; \theta) = \log(1 - \sigma_y(f(\psi(x^{adv}))). \tag{9}$$

Several optimization algorithms, such as the fast gradient sign method (Goodfellow et al., 2015) and projected gradient descent (Madry et al., 2018), have been commonly used for adversarial training. However, these algorithms aim to obtain the adversarial samples in the ℓ_∞ ball of the original samples, which cannot be directly applied to solving our problem. In our case, the interpolated adversarial samples are confined on the interpolated line of source data and target data. We propose a new optimization algorithm to solve the inner maximization optimization in Eq. (7). We initialize the interpolated adversarial samples with random λ and update them by back propagation in each iteration. The main procedures of our algorithm are summarized in Algorithm 1.

3.2.2 CLASS-IMBALANCED SEMANTIC CENTROID ALIGNMENT

Without careful control of the generation mechanism, the interpolated adversarial samples may not alleviate the issue of imbalanced class distribution. Moreover, although the interpolated adversarial

Algorithm 1 Solving the maximization problem in PAT

Input: Source samples from a mini-batch $\{(x_i^s, y_i^s)\}_{i=1}^{B_s}$, target samples and their pseudo labels $\{(x_i^t, \hat{y}_i^t)\}_{i=1}^{N_t}$, probability threshold of each class $\{P_k\}_{k=1}^{K}$
Output: Interpolated adversarial samples $\{\hat{x}_i^{adv}\}_{i=1}^{N_{adv}}$
  for each source sample x_i^s in the mini-batch **do**
    if rand() $> P_k(k = y_i^s)$ **then**
      Choose one target sample x_i^t with pseudo label equals to k
      Initialize x^{adv} with random λ using Eq. (6)
      repeat
        Calculates the gradient of λ with loss function in Eq. (7). $g_\lambda = \alpha \nabla_\lambda D'(x^{adv}, y; \theta)$
        Update λ with the gradient, $\lambda \leftarrow \lambda + g_\lambda$
        Clip the λ between 0 and 1, $\lambda \leftarrow \lambda \cdot \text{clip}(0, 1)$
        Update adversarial sample $\boldsymbol{x}^{adv}$ with new λ using Eq. (6).
      until the optimization converges
    end if
  end for

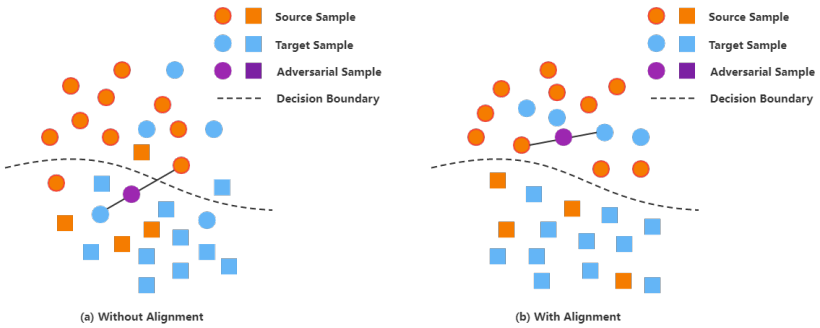

Figure 3: Illustration of generation of adversarial samples (a) without centroid alignment and (b) with centroid alignment. The adversarial samples generated without centroid alignment have a larger chance to violate the decision boundary.

samples bridge the source and target domains to some extent, the discrepancy between source and target domains is not explicitly reduced. To address these issues, we propose to explicitly align the source and target domains with imbalanced class distributions using two strategies.

First, we propose a strategy to guide the generation of interpolated adversarial samples. For training samples in each mini-batch from the source domain, they should not have the equal opportunity to generate interpolated adversarial samples. Since the decision boundary usually favors the majority classes, the probability of generating adversarial samples for minority classes should be larger than that for majority classes. For the k-th class, we set a probability threshold P_k as follows:

$$P_k = \frac{n_k}{n_{max} + \epsilon}, \tag{10}$$

where n_k is the number of the samples from the kth class. $n_{max} = \max_k \{n_k\}_{k=1}^{K}$, and ϵ is the bias. For a specific class, if a random number $r \in [0, 1)$ is larger than the corresponding threshold, the adversarial samples will be generated, as shown in Algorithm 1. We also adopt class-balanced sampling on the source data to alleviate the biased occurrence of the majority classes. Specifically, each class will be selected with an equal chance, in order to reduce the model prediction bias towards the majority classes.

Second, we incorporate the moving average centroid alignment (Xie et al., 2018) to align the conditional feature distributions of source and target domains by explicitly matching the centroids of two domains. As illustrated in Figure 3, without centroid alignment, the adversarial samples may be generated from a pair of samples in which one of the samples is misaligned to other classes, thus making the embedding of adversarial samples fall out of the decision boundary. With centroid alignment,

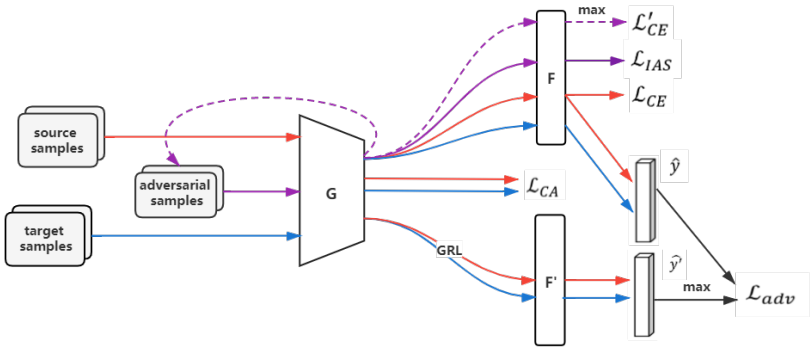

Figure 4: Illustration of our framework based on PAT and MDD. It includes a feature extractor G, an optimal classifier F, and an auxiliary classifier F'. The dashed line represents the data flow in pairwise adversarial training. The margin disparity discrepancy of two domains is diminished by aligning the two one-hot labels. We also explicitly align the pair of class conditioned samples by minimizing the distance of the centroids denoted as $\mathcal{L}_{CA}$.

we can eliminate the occurrence of such out-of-bound adversarial samples, and the interpolated adversarial samples could provide meaningful support for the minority class in the target domain. The loss function of moving average centroid alignment is defined as $\mathcal{L}_{CA} = \sum_{k=1}^{K} \text{dist}(\mathcal{C}_k^s, \mathcal{C}_k^t)$, where $\mathcal{C}_k^s$ and $\mathcal{C}_k^t$ denote the centroids of the kth class in the source domain and target domain, respectively. dist() can be implemented by the Euclidean distance or cosine distance.

3.3 PAT for Class Imbalanced Domain Adaptation

The proposed PAT approach could be integrated with many existing domain adaptation frameworks to enhance their performance on class-imbalanced data. In this paper, we adopt MDD (Zhang et al., 2019) as an example backbone model and showcase how to integrated PAT with it.

The MDD framework consists of a feature extractor G, an optimal classifier F, and an auxiliary classifier F'. The loss function of MDD is introduced in Eq. (1) and Eq. (2). Adversarial samples designed to maximize the modified cross-entropy function $\mathcal{L}'_{CE}$ are generated from the pair of source data and target data. Finally, the overall loss function of our framework is:

$$\mathcal{L} = \mathcal{L}_{MDD} + \alpha \mathcal{L}_{IAS} + \beta \mathcal{L}_{CA}, \tag{11}$$

where α and β are two trade-off parameters.

4 Experiments

In this section, we compare the performance of our approach with the state-of-the-art methods on class-imbalanced domain adaptation using three benchmark datasets.

4.1 Experimental Settings

Office-31 is a widely used benchmark image dataset for domain adaptation (Saenko et al., 2010). It contains 31 classes in three domains: Amazon (**A**), Dslr (**D**) and Webcam (**W**). The standard Office-31 doesn't exhibit obvious label distribution shift (LDS), so a new imbalanced Office-31 is created by sampling from standard ones as suggested by Tan et al. (2020). The distribution conforms to Paredo distribution (Reed, 2001) and follows the **R**eversely-unbalanced **S**ource and **U**nbalanced **T**arget **(RS-UT)** protocol. Both the source domain and target domain have shifted label distributions, and the label distribution of source domain is a reversed version of that of target domain. **Office-Home** is a large benchmark dataset containing 65 classes of objects commonly found in office and home scenarios (Venkateswara et al., 2017). It has four domains: Real-World (**Rw**), Clipart (**Cl**), Product (**Pr**) and Art (**Ar**). In our experiments, we use the existing imbalanced Office-Home with **RS-UT** distributions generated in Tan et al. (2020) to train and test our approach. Since there are

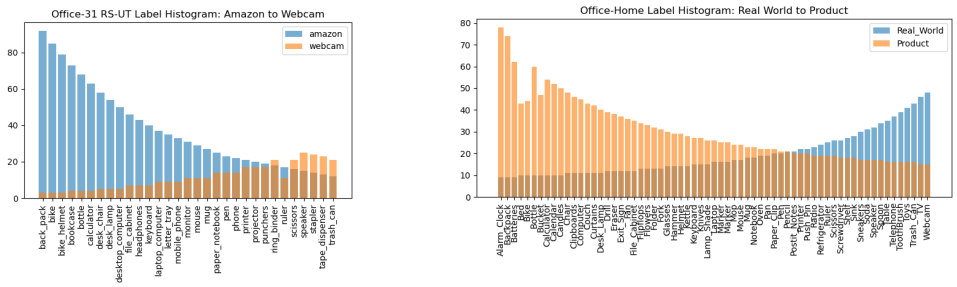

(a) Amazon→Webcam (b) Real_World→Product

Figure 5: (a) Biased label distribution shift on Amazon→Webcam from imbalanced Office-31. (b) Biased label distribution shift on Real_World→Product from imbalanced Office-Home.

Table 1: Per-class average accuracy on Office-Home dataset with RS→UT label shift. Bold and underscore denote the best and second-best performing methods, respectively.

Method	Rw→Pr	Rw→Cl	Pr→Rw	Pr→Cl	Cl→Rw	Cl→Pr	AVG
source †	70.74	44.24	67.33	38.68	53.51	51.85	54.39
BSP (Chen et al., 2019) †	72.80	23.82	66.19	20.05	32.59	30.36	40.97
PADA (Cao et al., 2018) †	60.77	32.28	57.09	26.76	40.71	38.34	42.66
BBSE (Lipton et al., 2018) †	61.10	33.27	62.66	31.15	39.70	38.08	44.33
MCD (Long et al., 2018) †	66.03	33.17	62.95	29.99	44.47	39.01	45.94
DAN (Long et al., 2015)	69.35	40.84	66.93	34.66	53.55	52.09	52.90
F-DANN (Wu et al., 2019) †	58.56	40.57	67.32	37.33	55.84	53.67	53.88
JAN (Long et al., 2017) †	67.20	43.60	68.87	39.21	57.98	48.57	54.24
DANN (Ganin & Lempitsky, 2015) †	71.62	46.51	68.40	38.07	58.83	58.05	56.91
MDD (Zhang et al., 2019) †	71.21	44.78	69.31	42.56	52.10	52.70	55.44
COAL (Tan et al., 2020) †	73.65	42.58	73.26	40.61	59.22	57.33	58.40
InstaPBM (Li et al., 2020) †	75.56	42.93	70.30	39.32	61,87	63.40	58.90
MDD+implicit (Jiang et al., 2020) †	76.08	50.04	74.21	45.38	61.15	63.15	61.67
SENTRY (Prabhu et al., 2021) †	76.12	**56.80**	73.60	**54.75**	65.94	64.29	65.25
Ours	**79.88**	54.68	**77.32**	50.21	**67.29**	**67.04**	**66.07**

† Data of the baseline methods are cited from Prabhu et al. (2021) .

very limited samples in the art (**Ar**) domain, we only conduct domain adaptation tasks on the other three domains. **DomainNet** is a large-scale benchmark dataset for domain adaptation (Peng et al., 2019). Since there are mislabeled samples in some classes and domains, we follow Tan et al. (2020) and adopt only 40 common classes from four domains: Real (**R**), Clipart (**C**), Painting (**P**), and Sketch (**S**). Different from Office-31 and Office-Home, the selected samples in DomainNet already exhibit obvious label distribution shift in the source domain and target domain. So there is no need to sample this dataset again. Figure 5 illustrates the label distributions of imbalanced Office31 and imbalanced Office-Home datasets.

We use PyTorch to implement our approach. We train our model with the mini-batch SGD, a Nesterov momentum of 0.9, and a weight decay of 0.0005. The learning rate of classifiers is 10 times larger than that of feature extractor, and all the learning rates are adjusted by every iteration. In order to obtain the interpolated adversarial sample from a pair of source sample and target sample from the same class, we utilize a memory pool to store the pseudo labels of all the target data. The pseudo labels are updated in every iteration. Note that we utilize a class-balanced sampler on the source data, which can be referred to as N-way (number of classes per batch) and K-shot (number of examples per class). The coefficient α is set to 0.5 and β is set to 0.05 for all the experiments. Following existing work on CDA, we adopt the per-class mean accuracy as our evaluation metric. All the experiments are implemented on Nvidia RTX A5000 platform.

4.2 COMPARISON WITH STATE-OF-ART CDA METHODS

We compare our approach with several state-of-art methods for class imbalanced domain adaptation. The baseline methods can be divided into two categories. The first category of methods are specif-

Table 2: Per-class average accuracy on DomainNet dataset. Bold and underscore denote the best and second-best performing methods respectively.

Method	R→C	R→P	R→S	C→R	C→P	C→S	P→R	P→C	P→S	S→R	S→C	S→P	AVG
source †	65.75	68.84	59.15	77.71	60.60	57.87	84.45	62.35	65.07	77.10	63.00	59.72	66.80
BBSE (Lipton et al., 2018) †	55.38	63.62	47.44	64.58	42.18	42.36	81.55	49.04	54.10	68.54	48.19	46.07	55.25
PADA (Cao et al., 2018) †	65.91	67.13	58.43	74.69	53.09	52.86	79.84	59.33	57.87	76.52	66.97	61.08	64.48
MCD (Long et al., 2018)†	61.97	69.33	56.26	79.78	56.61	53.66	83.38	58.31	60.98	81.74	56.27	66.78	65.42
DAN (Long et al., 2015) †	64.36	70.65	58.44	79.44	56.78	60.05	84.56	61.62	62.21	79.69	65.01	62.04	67.07
F-DANN (Wu et al., 2019) †	66.15	71.80	61.53	81.85	60.06	61.22	84.46	66.81	62.84	81.38	69.62	66.50	69.52
UAN (You et al., 2019) †	71.10	68.90	67.10	83.15	63.30	64.66	83.95	65.35	67.06	82.22	70.64	68.09	72.05
JAN (Long et al., 2017) †	65.57	73.58	67.61	85.02	64.96	67.17	87.06	67.92	66.10	84.54	72.77	67.51	72.48
ETN (Cao et al., 2019) †	69.22	72.14	63.63	86.54	65.33	63.34	85.04	65.69	68.78	84.93	72.17	68.99	73.99
BSP (Chen et al., 2019) †	67.29	73.47	69.31	86.50	67.52	70.90	86.83	70.33	68.75	84.34	72.40	71.47	74.09
DANN (Ganin & Lempitsky, 2015) †	63.37	73.56	72.63	86.47	65.73	70.58	86.94	73.19	70.15	85.73	75.16	70.04	74.46
COAL (Tan et al., 2020) †	73.58	75.37	70.50	89.63	69.98	71.29	89.81	68.01	70.49	87.97	73.21	70.53	75.89
MDD+implicit	75.54	74.30	70.02	88.17	70.50	70.30	87.94	72.03	72.29	88.85	76.12	71.21	76.44
InstaPBM (Li et al., 2020) †	80.10	75.87	70.84	89.67	70.21	72.76	89.60	74.41	72.19	87.00	79.66	71.75	77.84
Sentry (Prabhu et al., 2021) †	**83.89**	76.72	74.43	**90.61**	**76.02**	**79.47**	**90.27**	**82.91**	75.60	**90.41**	**82.40**	73.98	**81.39**
Ours	80.15	**76.93**	**76.08**	89.87	72.25	76.25	90.04	79.11	**76.32**	89.61	80.71	**75.46**	80.23

† Data of the baseline methods are cited from Prabhu et al. (2021)

Table 3: Per-class average accuracy on Office-31 with RS→UT label shift. Bold and underscore denote the best and second-best performing methods respectively.

Method	A→W	D→W	W→D	A→D	D→A	W→A	AVG
source	71.77	90.86	93.06	72.25	59.03	58.34	74.21
F-DANN (Wu et al., 2019)	69.83	93.56	93.95	76.45	58.57	58.11	75.07
Sentry (Prabhu et al., 2021)	81.77	90.95	93.50	83.91	62.72	64.00	79.48
COAL (Tan et al., 2020)	81.18	91.12	95.46	81.67	66.08	66.60	80.35
MDD+implicit (Jiang et al., 2020)	85.79	**96.20**	**97.40**	84.25	68.11	66.63	83.06
Ours	**89.61**	96.08	97.08	**86.66**	**71.93**	**70.40**	**85.29**

ically designed to solve the CDA problem, including Sentry (Prabhu et al., 2021), MDD+implicit Jiang et al. (2020), COAL (Tan et al., 2020), and F-DANN (Wu et al., 2019). The second category of methods aim to solve the standard unsupervised domain adaptation problem, including the InstaPBM (Li et al., 2020) and BSP (Chen et al., 2019).

Table 1 shows the per-class average accuracy and overall average accuracy of our approach and baselines on the imbalanced Office-Home dataset. The results of the baseline are cited from Prabhu et al. (2021). Our proposed model achieves the best results in 4 out of 6 tasks. The accuracies of our approach in these 4 tasks are more than 3% higher than the second-best results. In addition, our model obtains the second-best results in the Rw→CL and Pr→Cl tasks. Overall, our method achieves the highest average accuracy (i.e., 66.07%) among all the compared methods.

Table 2 shows the per-class average accuracies of our approach and baselines on the DomainNet dataset. Our approach achieves the best results in 4 tasks and second-best results in 8 tasks. In R→S, P→S and S→P, our model can achieve 76.08%, 75.46%, which are 1.65% and 1.48% higher than the second-best results, respectively. Though in some tasks our results are lower than Sentry (Prabhu et al., 2021), the overall average accuracy of our approach is comparable to that of Sentry.

We manually sample the standard Office-31 dataset and construct the imbalanced Office-31 dataset, in which the label distribution conforms to the Paredo distribution (Reed, 2001). We compare our model with current state-of-art methods that focus on the CDA problem. Among all the 6 tasks, our model achieves best results in 4 tasks. In these tasks, our results are 3.82%, 2.41%, 3.28% and 3.77% higher than the second best results. In the D→W and W→D tasks, the performance of our approach are only 0.12% and 0.32% less than the best results.

4.3 ABLATION STUDIES

We further investigate the performance of our approach from two aspects. First, we evaluate the contribution of each component in the loss function. Second, we evaluate the effect of the number

Table 4: Per-class average accuracy of MDD, Ours w/o IAS, Ours w/o CA, and our full model on three tasks from imbalanced Office-Home dataset. Bold denotes the best performing method.

Method	Rw→Pr	Pr→Cl	Cl→Pr	AVG
MDD (baseline) †	75.96	42.73	58.76	59.15
Ours w/o IAS †	78.38	48.31	65.80	64.16
Ours w/o CA †	77.37	47.08	64.73	63.06
Ours †	**79.88**	**50.21**	**67.04**	**65.71**

† We adopt class-balanced source sampling on all these methods.

of the iteration in the inner maximization of pairwise adversarial training. At last, we evaluate the sensitivity of the model to the change of the hyper-parameters.

The proposed pairwise adversarial training approach includes two major components, i.e., interpolated adversarial samples (IAS) and centroid alignment (CA). We choose three tasks from each of the three datasets separately. Table 4 shows the performance of our backbone model MDD, Ours w/o IAS, Ours w/o CA, and our full model on the imbalanced Office-Home dataset. Detailed results on the other two datasets are provided in the Appendix. Ours w/o IAS and Ours w/o CA consistently achieve better performance than the baseline model MDD, which validates the effectiveness of both methods in dealing with the biased label distribution shift. Our full model further improves the classification accuracy, demonstrating the complementary roles of pairwise adversarial samples and centroid alignment in our approach.

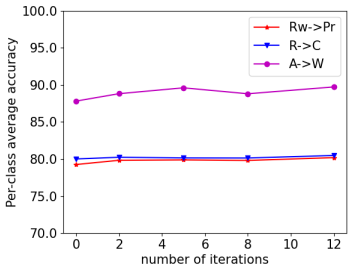

Figure 6: Per-class average accuracy of our model with different number of iterations in three tasks.

We also evaluate the effect of the number of iterations of the inner maximization in pairwise adversarial training. We choose Rw→Pr from Office-Home, R→C from DomainNet and A→W from Office-31 as our evaluation tasks. The results are illustrated in Figure 6. It shows that the performance of our approach will generally increase with more iterations. At some points the performance experiences the slight fluctuation. Though performance reaches the maximum value at iteration of 12, it is relatively time-consuming in the training process.

Furthermore, we evaluate the sensitivity of our model to the change of two hyperparameters α and β . In particular, we first set β to 0.05 and choose α from $[0, 2.5]$. Then, α is set to 0.5, and β is chosen from $[0, 0.25]$. Figure 7 shows the per-class average accuracy of our model when varying the hyperparameter values. It shows that our model is not very sensitive to the settings of hyper-parameters in a relatively wide range.

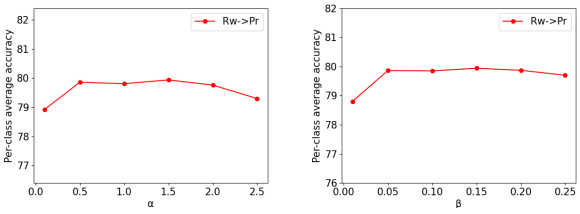

(a) (b)

Figure 7: Average accuracy of our model with: (a) varying α when $\beta = 0.05$, and (b) varying β when $\alpha = 0.5$ on Rw→Pr in imbalanced Office-Home.

5 Conclusion

In this paper, we propose a pairwise adversarial training approach to tackle the class-imbalanced unsupervised domain adaptation (CDA) problem. Our approach generates interpolated adversarial samples across source and target domains. In order to alleviate the biased label distribution shift issue, we use the interpolated adversarial samples to augment the training data (especially the minority classes) and meanwhile adopt the centroid alignment strategy to explicitly align source and target domains. Experimental results on three CDA benchmark datasets show that, our approach yields competing performance compared with state-of-art CDA methods.

REFERENCES

Yogesh Balaji, Rama Chellappa, and Soheil Feizi. Normalized wasserstein for mixture distributions with applications in adversarial learning and domain adaptation. In *Proceedings of the IEEE/CVF International Conference on Computer Vision*, pp. 6500–6508, 2019.

Zhangjie Cao, Lijia Ma, Mingsheng Long, and Jianmin Wang. Partial adversarial domain adaptation. In *Proceedings of the European Conference on Computer Vision (ECCV)*, pp. 135–150, 2018.

Zhangjie Cao, Kaichao You, Mingsheng Long, Jianmin Wang, and Qiang Yang. Learning to transfer examples for partial domain adaptation. In *CVPR*, pp. 2985–2994. Computer Vision Foundation / IEEE, 2019.

Nitesh V. Chawla, Kevin W. Bowyer, Lawrence O. Hall, and W. Philip Kegelmeyer. SMOTE: synthetic minority over-sampling technique. *J. Artif. Intell. Res.*, 16:321–357, 2002.

Xinyang Chen, Sinan Wang, Mingsheng Long, and Jianmin Wang. Transferability vs. discriminability: Batch spectral penalization for adversarial domain adaptation. In *ICML*, volume 97 of *Proceedings of Machine Learning Research*, pp. 1081–1090. PMLR, 2019.

Hsin-Ping Chou, Shih-Chieh Chang, Jia-Yu Pan, Wei Wei, and Da-Cheng Juan. Remix: Rebalanced mixup. In *ECCV Workshops (6)*, volume 12540 of *Lecture Notes in Computer Science*, pp. 95–110. Springer, 2020.

Zhijie Deng, Yucen Luo, and Jun Zhu. Cluster alignment with a teacher for unsupervised domain adaptation. In *Proceedings of the IEEE/CVF International Conference on Computer Vision*, pp. 9944–9953, 2019.

Yaroslav Ganin and Victor S. Lempitsky. Unsupervised domain adaptation by backpropagation. In *ICML*, volume 37 of *JMLR Workshop and Conference Proceedings*, pp. 1180–1189. JMLR.org, 2015.

Yaroslav Ganin, Evgeniya Ustinova, Hana Ajakan, Pascal Germain, Hugo Larochelle, François Laviolette, Mario Marchand, and Victor Lempitsky. Domain-adversarial training of neural networks. *The journal of machine learning research*, 17(1):2096–2030, 2016.

Ian J. Goodfellow, Jean Pouget-Abadie, Mehdi Mirza, Bing Xu, David Warde-Farley, Sherjil Ozair, Aaron C. Courville, and Yoshua Bengio. Generative adversarial nets. In *NIPS*, pp. 2672–2680, 2014.

Ian J. Goodfellow, Jonathon Shlens, and Christian Szegedy. Explaining and harnessing adversarial examples. In *ICLR (Poster)*, 2015.

Chuan Guo, Geoff Pleiss, Yu Sun, and Kilian Q. Weinberger. On calibration of modern neural networks. In *ICML*, volume 70 of *Proceedings of Machine Learning Research*, pp. 1321–1330. PMLR, 2017.

Agrim Gupta, Piotr Dollár, and Ross B. Girshick. LVIS: A dataset for large vocabulary instance segmentation. In *CVPR*, pp. 5356–5364. Computer Vision Foundation / IEEE, 2019.

Xiang Jiang, Qicheng Lao, Stan Matwin, and Mohammad Havaei. Implicit class-conditioned domain alignment for unsupervised domain adaptation. In *International Conference on Machine Learning*, pp. 4816–4827. PMLR, 2020.

Guoliang Kang, Lu Jiang, Yi Yang, and Alexander G Hauptmann. Contrastive adaptation network for unsupervised domain adaptation. In *Proceedings of the IEEE/CVF Conference on Computer Vision and Pattern Recognition*, pp. 4893–4902, 2019.

Jaeho Lee and Maxim Raginsky. Minimax statistical learning with wasserstein distances. *Advances in Neural Information Processing Systems*, 2018:2687–2696, 2018.

Bo Li, Yezhen Wang, Tong Che, Shanghang Zhang, Sicheng Zhao, Pengfei Xu, Wei Zhou, Yoshua Bengio, and Kurt Keutzer. Rethinking distributional matching based domain adaptation. *CoRR*, abs/2006.13352, 2020.

Tsung-Yi Lin, Michael Maire, Serge J. Belongie, James Hays, Pietro Perona, Deva Ramanan, Piotr Dollár, and C. Lawrence Zitnick. Microsoft COCO: common objects in context. In *ECCV (5)*, volume 8693 of *Lecture Notes in Computer Science*, pp. 740–755. Springer, 2014.

Zachary Lipton, Yu-Xiang Wang, and Alexander Smola. Detecting and correcting for label shift with black box predictors. In *International conference on machine learning*, pp. 3122–3130. PMLR, 2018.

Mingsheng Long, Yue Cao, Jianmin Wang, and Michael I. Jordan. Learning transferable features with deep adaptation networks. In *ICML*, volume 37 of *JMLR Workshop and Conference Proceedings*, pp. 97–105. JMLR.org, 2015.

Mingsheng Long, Han Zhu, Jianmin Wang, and Michael I Jordan. Unsupervised domain adaptation with residual transfer networks. *Advances in Neural Information Processing Systems*, 29:136–144, 2016.

Mingsheng Long, Han Zhu, Jianmin Wang, and Michael I Jordan. Deep transfer learning with joint adaptation networks. In *International conference on machine learning*, pp. 2208–2217. PMLR, 2017.

Mingsheng Long, Zhangjie Cao, Jianmin Wang, and Michael I. Jordan. Conditional adversarial domain adaptation. In *NeurIPS*, pp. 1647–1657, 2018.

Aleksander Madry, Aleksandar Makelov, Ludwig Schmidt, Dimitris Tsipras, and Adrian Vladu. Towards deep learning models resistant to adversarial attacks. In *ICLR (Poster)*. OpenReview.net, 2018.

Takeru Miyato, Shin-ichi Maeda, Masanori Koyama, and Shin Ishii. Virtual adversarial training: a regularization method for supervised and semi-supervised learning. *IEEE transactions on pattern analysis and machine intelligence*, 41(8):1979–1993, 2018.

Zhongyi Pei, Zhangjie Cao, Mingsheng Long, and Jianmin Wang. Multi-adversarial domain adaptation. In *Thirty-second AAAI conference on artificial intelligence*, 2018.

Xingchao Peng, Qinxun Bai, Xide Xia, Zijun Huang, Kate Saenko, and Bo Wang. Moment matching for multi-source domain adaptation. In *ICCV*, pp. 1406–1415. IEEE, 2019.

Viraj Prabhu, Shivam Khare, Deeksha Karthik, and Judy Hoffman. Selective entropy optimization via committee consistency for unsupervised domain adaptation. In *International Conference in Computer Vision (ICCV)*, 2021.

William J Reed. The pareto, zipf and other power laws. *Economics letters*, 74(1):15–19, 2001.

Kate Saenko, Brian Kulis, Mario Fritz, and Trevor Darrell. Adapting visual category models to new domains. In *ECCV (4)*, volume 6314 of *Lecture Notes in Computer Science*, pp. 213–226. Springer, 2010.

Kuniaki Saito, Kohei Watanabe, Yoshitaka Ushiku, and Tatsuya Harada. Maximum classifier discrepancy for unsupervised domain adaptation. In *Proceedings of the IEEE conference on computer vision and pattern recognition*, pp. 3723–3732, 2018.

Jian Shen, Yanru Qu, Weinan Zhang, and Yong Yu. Wasserstein distance guided representation learning for domain adaptation. In *Thirty-Second AAAI Conference on Artificial Intelligence*, 2018.

Rui Shu, Hung Bui, Hirokazu Narui, and Stefano Ermon. A dirt-t approach to unsupervised domain adaptation. In *International Conference on Learning Representations*, 2018.

Baochen Sun and Kate Saenko. Deep coral: Correlation alignment for deep domain adaptation. In *European conference on computer vision*, pp. 443–450. Springer, 2016.

Christian Szegedy, Wojciech Zaremba, Ilya Sutskever, Joan Bruna, Dumitru Erhan, Ian Goodfellow, and Rob Fergus. Intriguing properties of neural networks. In *2nd International Conference on Learning Representations, ICLR 2014*, 2014.

Shuhan Tan, Xingchao Peng, and Kate Saenko. Class-imbalanced domain adaptation: an empirical odyssey. In *European Conference on Computer Vision*, pp. 585–602. Springer, 2020.

Hemanth Venkateswara, Jose Eusebio, Shayok Chakraborty, and Sethuraman Panchanathan. Deep hashing network for unsupervised domain adaptation. In *CVPR*, pp. 5385–5394. IEEE Computer Society, 2017.

Yifan Wu, Ezra Winston, Divyansh Kaushik, and Zachary Lipton. Domain adaptation with asymmetrically-relaxed distribution alignment. In *International Conference on Machine Learning*, pp. 6872–6881. PMLR, 2019.

Shaoan Xie, Zibin Zheng, Liang Chen, and Chuan Chen. Learning semantic representations for unsupervised domain adaptation. In *ICML*, volume 80 of *Proceedings of Machine Learning Research*, pp. 5419–5428. PMLR, 2018.

Kaichao You, Mingsheng Long, Zhangjie Cao, Jianmin Wang, and Michael I. Jordan. Universal domain adaptation. In *CVPR*, pp. 2720–2729. Computer Vision Foundation / IEEE, 2019.

Chaohui Yu, Jindong Wang, Yiqiang Chen, and Meiyu Huang. Transfer learning with dynamic adversarial adaptation network. In *2019 IEEE International Conference on Data Mining (ICDM)*, pp. 778–786. IEEE, 2019.

Yuchen Zhang, Tianle Liu, Mingsheng Long, and Michael I. Jordan. Bridging theory and algorithm for domain adaptation. In *ICML*, volume 97 of *Proceedings of Machine Learning Research*, pp. 7404–7413. PMLR, 2019.

A APPENDIX

Table 5 and Table 6 show the per-class average accuracy of MDD, Ours w/o IAS, Ours w/o CA, and our full model on three tasks from the DomainNet dataset and Office-31 dataset, respectively. The results demonstrate the effectiveness of two major components (i.e., interpolated adversarial samples and centroid alignment) in our approach.

Table 5: Per-class average accuracy of MDD, Ours w/o IAS, Ours w/o CA, and our full model on three tasks from DomainNet dataset. Bold denotes the best performing method.

Method	R→C	C→P	C→R	AVG
MDD (baseline) †	75.30	70.38	87.94	77.87
Ours w/o IAS †	77.03	69.43	88.60	78.35
Ours w/o CA †	77.65	71.25	88.49	79.13
Ours †	**80.15**	**72.25**	**89.87**	**80.76**

† We adopt class-balanced source sampling on all these methods.

Table 6: Per-class average accuracy of MDD, Ours w/o IAS, Ours w/o CA, and our full model on imbalanced Office-31 dataset. Bold denotes the best performing method.

Method	A→W	W→D	W→A	AVG
MDD (baseline) †	85.86	96.12	65.20	82.39
Ours w/o IAS †	87.41	96.44	68.42	84.09
Ours w/o CA †	**90.58**	96.55	69.99	85.71
Ours †	89.61	**97.08**	**70.04**	**85.58**

† We adopt class-balanced source sampling on all these methods.